

Multiplicity Distributions in Pseudorapidity Intervals with ^{32}S at 200 GeV/nucleon and ^{16}O at 200 and 60 GeV/nucleon

G. Singh, K. Sengupta, and P. L. Jain

High Energy Experimental Laboratory, Department of Physics, State University of New York at Buffalo, Buffalo, New York 14260

(Received 25 April 1988)

We present results of our systematic studies of charged-shower-particle multiplicities and their dependence on pseudorapidity intervals for nearly central events produced by ^{32}S at 200 GeV/nucleon and ^{16}O at 200 and 60 GeV/nucleon in nuclear emulsion. An increase in the particle density with the increase of particle energy and mass is observed. We find an energy-independent linear relation between the maximum particle density (in a given pseudorapidity interval) and shower-particle multiplicity.

PACS numbers: 25.70.Np

The general dynamics of hadron-hadron interactions at very high energies is reasonably well understood as compared to hadron-nucleus interactions. The least understood is, however, the dynamics of nucleus-nucleus collisions, which is by far the most complex of the three. Relatively speaking, very little systematic work has been done in the field of ultrarelativistic nucleus-nucleus collisions since there was no high-energy heavy-ion accelerator (>100 GeV/nucleon) available prior to the year 1986. The only source of high-energy particles had been cosmic rays, but these are not monoenergetic. It was only in the later parts of the years 1986 and 1987 that ^{16}O and ^{32}S ions were accelerated to 200 GeV/nucleon at CERN. The special feature which distinguishes nucleus-nucleus collisions from the other two kinds is that in the former case a large amount of energy is released because of numerous nucleon-nucleon interactions and multiple scatterings of the constituents within the nuclear dimensions. Lattice QCD calculations¹ predict that in central collisions of heavy nuclei, energy densities of the order of a few GeV/fm³ can be reached over a large interaction volume and a transition to a new phase of matter such as a quark-gluon plasma may take place.

Recently, a number of theoretical models² have been built on the basis of different hypotheses for the production of shower particles in nucleus-nucleus collisions at ultrarelativistic energies. The experimental parameter which seems to be very important in the theoretical models is the pseudorapidity-interval ($\Delta\eta_L$) dependence of the multiplicity distribution of shower particles. In this Letter, we present for the first time systematic studies of this parameter in nearly central events (defined in Ref. 3) produced in nuclear emulsion by beams of ^{32}S (beam *A*) and ^{16}O (beam *B*) at 200 GeV/nucleon and ^{16}O (beam *C*) at 60 GeV/nucleon.

The details of our experiment with beam *B* are reported in Ref. 3. The same procedure applies to beams *A* and *C* as well. For the present investigation, we selected 124, 191, and 153 nearly central events of beams *A*, *B*,

and *C*, respectively. After elimination of the elastic and electromagnetic dissociated events, the mean free paths are found to be $\lambda_A = 10.01 \pm 0.52$ cm, $\lambda_B = 11.45 \pm 0.84$ cm, and $\lambda_C = 12.01 \pm 1.03$ cm for 37, 23, and 20 m of track lengths of the respective beams. For beams *A*, *B*, and *C*, the average multiplicities, $\langle n_s \rangle$, and the $D/\langle n_s \rangle$ ratios are 222 ± 20 , 0.39 ± 0.03 ; 120 ± 9 , 0.51 ± 0.04 ; 82 ± 7 , 0.43 ± 0.04 , respectively. For the same projectile mass, the multiplicity of shower particles is seen to vary with projectile energy according to the relation $\langle n_s \rangle = aE^\alpha$. For beams *B* and *C*, the parameters a and α have values 20.95 and 0.33, respectively. With use of these values of a and α , the shower-particle multiplicity for the 14-GeV/nucleon ^{16}O beam was estimated to be ≈ 50 , which is in agreement with $\langle n_s \rangle = 49.3$, as reported in Ref. 4. This general law has also been used in cosmic-ray studies.⁵

In Fig. 1(a) are shown the frequencies of nearly central events plotted against their multiplicities. The normalized pseudorapidity distributions $(dn/d\eta_L)/N_{ev}$ of charged shower particles are shown in Fig. 1(b). The heights and widths of the plateaus increase with the increase in the energy and mass of the projectile. For beams *B* and *C*, there is an approximate scaling in the target-fragmentation region up to $\eta_L \leq 1.4$. This scaling is demonstrated in Fig. 1(c), where the charged-particle density per unit of pseudorapidity, $\langle dn/d\eta_L \rangle$ ($=\langle \rho \rangle$), is plotted against the multiplicity in the target-fragmentation region for beams *B* and *C*. Both curves have approximately the same slopes.

Events in multiparticle production with a large concentration of particles in small rapidity windows have been known for a long time.⁶ Recently, an interest in large fluctuations in rapidity was revived because of well known predictions that it may indicate possible signals of quark-gluon plasma formation. Multiplicity distributions have different shapes in different pseudorapidity intervals, although they are quite symmetric about the center. We have calculated the average density of charged particles $\langle \rho \rangle$ in pseudorapidity intervals ($2\eta_w$,

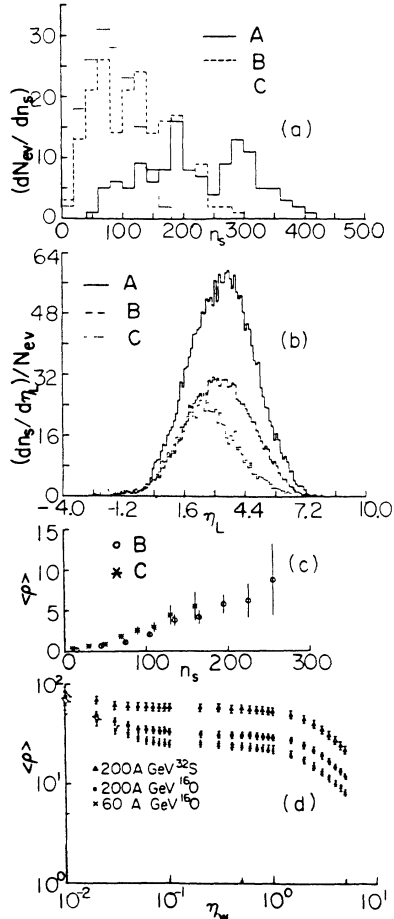


FIG. 1. (a) The charged-shower-particle multiplicity distributions for central events. (b) Normalized pseudorapidity (η_L) distributions for charged shower particles. (c) Average charged-particle density (excluding evaporation prongs) per unit pseudorapidity, $\langle \rho \rangle$, plotted as a function of the number of shower particles in the target-fragmentation region of pseudorapidity ($\eta_L \leq 1.4$) for beams *B* and *C*. (d) Plot of $\langle \rho \rangle$ at different pseudorapidity intervals, η_w , chosen symmetrically about the center of symmetry of the full rapidity spectrum. Beam *A*, 200-GeV/nucleon ^{32}S ; beam *B*, 200-GeV/nucleon ^{16}O ; beam *C*, 60-GeV/nucleon ^{16}O .

where $0.1 \leq \eta_w \leq 5$) of increasing width, placed symmetrically about the center of symmetry of the full rapidity spectrum. Then $\langle \rho \rangle$ is plotted for beams *A*, *B*, and *C* as a function of η_w in Fig. 1(d). The plateaus of these curves, which correspond to the central regions of the relevant pseudorapidity distributions, have widths and heights which increase with beam energy and projectile mass. The average shower-particle densities $\langle \rho \rangle$ in the central regions for beams *A*, *B*, and *C* are 58.0 ± 5.2 , 32.7 ± 2.4 , and 26.1 ± 2.1 , respectively.

Rapidity density reflects entropy density. In general, a concentration of particles in rapidity is associated with a random azimuthal-angle distribution and events with large fluctuations do not show jetlike structures. In Fig.

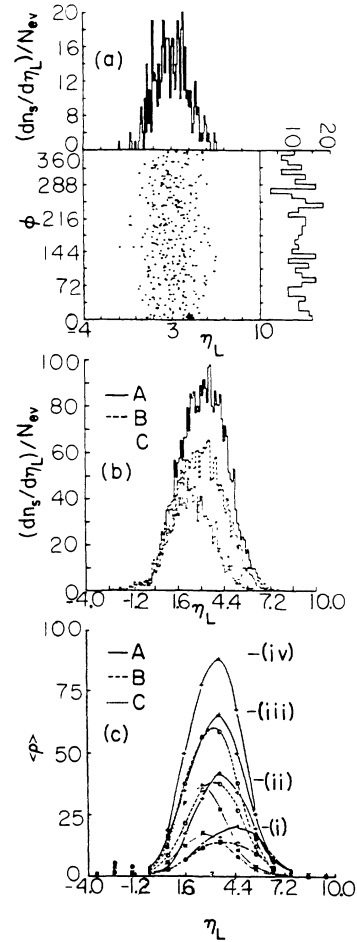


FIG. 2. (a) Pseudorapidity (η_L) and azimuthal-angle (ϕ) distributions for a selected ^{32}S -AgBr event ($n_s = 403$). (b) Normalized pseudorapidity (η_L) distributions of charged particles for events with very large multiplicities: $n_s \geq 300$ for beam *A*, $n_s \geq 200$ for beam *B*, and $n_s \geq 125$ for beam *C*. (c) Plot of $\langle \rho \rangle$ vs η_L at different multiplicity intervals: (i) $n_s < 100$, (ii) $100 \leq n_s < 200$, (iii) $200 \leq n_s < 300$, and (iv) $n_s \geq 300$. Beam *A*, plusses; beam *B*, circles; beam *C*, asterisks. The points have been connected by hand-drawn curves to guide the eye. Statistical errors are not shown here to avoid the confusion. Beam *A*, 200-GeV/nucleon ^{32}S ; beam *B*, 200-GeV/nucleon ^{16}O ; beam *C*, 60-GeV/nucleon ^{16}O .

2(a), the η_L distribution and the correlation of n_s with the azimuthal angle (ϕ) of the event having the highest multiplicity in our sample ($n_s = 403$) are shown for beam *A*. Most of the central events have almost uniform azimuthal-angle distributions for produced particles over the full η_L range. The individual bubbles like the ones shown in Fig. 2(a) are smeared out in the overall η_L distribution, as shown in Fig. 1(b). There are 27, 22, and 20 central events in our sample having the highest multiplicities: $n_s \geq 300$, 200, and 125 produced by beams *A*, *B*, and *C*, respectively. The overall pseudorapidity distributions of these events are shown in Fig. 2(b). The par-

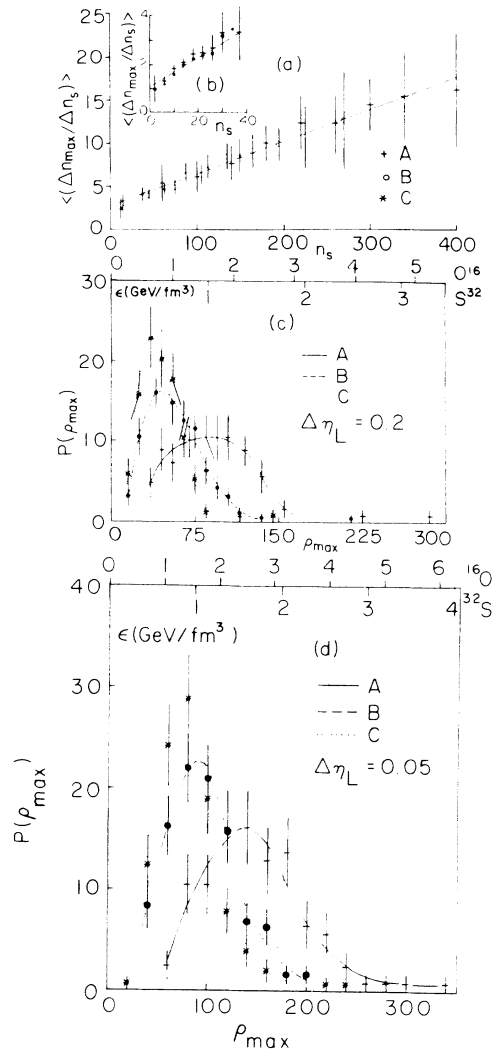


FIG. 3. The average of the maximum number of charged particles, $\langle \Delta n_{\max} / \Delta n_s \rangle$, as a function of the number of shower particles (n_s) for (a) beams *A*, *B*, and *C*. (b) Protons at 800 (pluses) and 400 (filled circles) GeV. Statistical errors are shown for the 800-GeV data only. Data points have been approximated with least-squared-fitted straight lines. Δn_{\max} was determined by scanning of each event with a fixed pseudorapidity window of width $\Delta\eta_L = 0.1$ unit. (c),(d) Maximum charged-particle-density (ρ_{\max}) distributions for beams *A*, *B*, and *C*. The pseudorapidity window widths chosen here are $\Delta\eta_L = 0.2$ and 0.05 unit, respectively. The upper axes show the calculated energy density (ϵ) for beams *A* and *B* separately, using Bjorken's relation (Ref. 8). The data points are connected by hand-drawn curves. Beam *A*, 200-GeV/nucleon ^{32}S ; beam *B*, 200-GeV/nucleon ^{16}O ; beam *C*, 60-GeV/nucleon ^{16}O .

ticle densities for the three beams are 84.23 ± 16.2 , 57.36 ± 12.2 , and 38.68 ± 8.7 , respectively.

We now divide all the events from beams *A*, *B*, and *C* into four different groups of multiplicity: $n_s < 100$, $100 \leq n_s < 200$, $200 \leq n_s < 300$, and $n_s \geq 300$. The plot of average particle density per unit of pseudorapidity (ρ)

versus η_L is shown for beams *A*, *B*, and *C* in Fig. 2(c). At all the energies the distributions are Gaussian in shape and in each case a forward shift of the peak is observed with the increase in projectile mass. For similar multiplicities from the same projectiles at different energies, the height of the peak is almost the same, but is shifted towards the midrapidity region with the increase in energy. From these figures, it is clear that for the same multiplicities the peak values of $\langle \rho \rangle$ are almost the same for similar projectiles, indicating that the particle density depends only upon the multiplicity (n_s) and not upon the projectile energy.

Recently, there has been a great deal of interest in measurement of the high-density fluctuations of particle production in pseudorapidity space.⁷ So, instead of an average particle density, we now determine the maximum number of particles in each event by scanning with a fixed pseudorapidity window of width $\Delta\eta_L = 0.1$ unit across its full rapidity range. The average of this quantity, $\langle \Delta n_{\max} / \Delta n_s \rangle$, is plotted in Fig. 3(a) as a function of the multiplicity bins Δn_s for all the three beams. The least-squares fit to the data is of the form $A + Bn_s$, where the intercept $A = 2.62 \pm 0.22$ and the slope $B = 0.038 \pm 0.001$. Our data show that the maximum number of particles in a given pseudorapidity interval increases linearly with multiplicity and is independent of the projectile masses and their energies. This maximum number of particles demonstrates scaling which can be very useful for future studies. For the sake of comparison, we also show in Fig. 3(b) [inset in Fig. 3(a)], the same distribution for proton beams of energies 400 and 800 GeV in nuclear emulsion,⁹ using a pseudorapidity window of size $\Delta\eta_L = 0.1$. This distribution for proton-nucleus collisions is also linear and energy independent. Finally, in Figs. 3(c) and 3(d), we present the probability of observing a given maximum particle density ρ_{\max} for all the three beams using intervals $\Delta\eta_L = 0.2$ and $\Delta\eta_L = 0.05$, respectively. The tails of these distributions extend as a function of the beam energy. For the highest-multiplicity events of beams *A* and *B*, the calculated values of energy densities reach ~ 3 and $\sim 4 \text{ GeV}/\text{fm}^3$, indicating a possibility of observing a new state of matter (quark-gluon plasma).

We conclude that for nearly central collisions, the particle density with the same projectile mass depends only upon the multiplicity and not upon the energy. The maximum particle density in a given pseudorapidity interval increases linearly with charged-particle multiplicity and is independent of the energy and mass of the projectile.

We thank Professor G. Vanderhaeghe, the CERN technical staff, and the emulsion operating group for their help in the exposure and development of our emulsion stacks. We are also thankful to Professor G. Romano for his generous help. This research work was supported in part by the National Science Foundation under

Grant No. NFS/PHY 8614797.

¹L. McLerran and B. Svetitsky, Phys. Lett. **98B**, 195 (1981); T. Celik, J. Engels, and H. Satz, Nucl. Phys. **B256**, 670 (1985); *Quark Matter Formation and Heavy Ion Collisions: Proceedings of the Bielefeld Workshop, 10-14 May 1982*, edited by M. Jacob and H. Satz (World Scientific, Singapore, 1982).

²L. Van Hove, Z. Phys. C **27**, 135 (1985); Larry McLerran, Fermilab Report No. Conf. 86/164-T, 1986 (unpublished); C. Y. Wong, Phys. Rev. D **30**, 961 (1984); H. Satz, in *Proceedings of the Twenty-Third International Conference on*

High Energy Physics, Berkeley, California, 1986, edited by S. Loken (World Scientific, Singapore, 1987).

³P. L. Jain, K. Sengupta, and G. Singh, Phys. Rev. Lett. **59**, 2531 (1987).

⁴L. M. Barbier *et al.*, Phys. Rev. Lett. **60**, 405 (1988).

⁵P. L. Jain, E. Loharmann, and M. W. Teucher, Phys. Rev. **115**, 643 (1959); M. W. Teucher *et al.*, Phys. Rev. **111**, 1384 (1958).

⁶P. L. Jain, Phys. Rev. **122**, 1891 (1961), and Nuovo Cimento **24**, 698 (1962).

⁷T. H. Burnett *et al.*, Phys. Rev. Lett. **50**, 2062 (1983).

⁸J. D. Bjorken, Phys. Rev. D **27**, 140 (1983).

⁹P. L. Jain, K. Sengupta, and G. Singh, Phys. Lett. B **187**, 175 (1987), and Phys. Rev. D **34**, 2886 (1986); P. L. Jain, Phys. Rev. **125**, 679 (1962).